Journal of Hazardous Materials 173 (2010) 462–467

Contents lists available at ScienceDirect

Journal of Hazardous Materials

journal homepage: www.elsevier.com/locate/jhazmat

# Batch and column separation characteristics of copper-imprinted porous polymer micro-beads synthesized by a direct imprinting method

Nguyen To Hoai, Dong-Keun Yoo, Dukjoon Kim *

*Department of Chemical Engineering, Polymer Technology Institute, Sungkyunkwan University, Suwon, Kyunggi, 440-746, South Korea*

ARTICLE INFO

*Article history:*
Received 12 March 2009
Received in revised form 21 August 2009
Accepted 22 August 2009
Available online 31 August 2009

*Keywords:*
Imprinted polymer
Selective separation
Heavy metal ion
Metal/monomer complex

ABSTRACT

Copper (II) ion-imprinted porous polymethacrylate micro-particles were prepared. Two functional monomers, methacrylic acid and vinyl pyridine, formed a complex with the template copper ion through ionic interactions. The self-assembled copper/monomer complex was polymerized in the presence of an ethylene glycol dimethacrylate cross-linker by a suspension method. After the imprinting sites were provided through removal of the template, the micro-porous particles, of approximate size 200 μm, were obtained for batch and column separation applications. The chemical structure and morphology of the Cu(II)-imprinted micro-porous particles were analyzed using FTIR, SEM, and BET. The adsorption capacity and adsorption kinetics of the imprinted beads for the template Cu(II) ion were significantly affected by particle size, copper ion concentration, pH, and flow rate of the feed solution. The imprinted particles showed high selectivity for the copper ion over other metal ions such as Ni and Zn. The selectivity of the present imprinted polymers for the copper ion was at least 10 times as high as those from commercial sources.



## 1. Introduction

Currently, the treatment of industry waste has been a strong concern as it continues to develop. One category of industrial pollutants includes heavy metals, often contained in the wastewater, such as copper, nickel, zinc, arsenic, and palladium. When released into the environment, these heavy metals can cause severe damage to the human body, including accumulative poison, brain damage, and cancer.

Several processes are currently in place for heavy metal removal, including chemical precipitation, membrane, and ion exchange [1–13]. In chemical precipitation, the heavy metals are removed by precipitation in solution as salts. The metal ions can also be separated by membranes using both their barrier structures and properties associated with a variety of unique morphologies and physicochemical interactions between membranes and metal ions. In ion exchange, the positively charged metal ions are exchanged with proton or sodium ions within anionic or chelating groups contained in resins. While these methods are industrially applicable for non-preferential separation, the inherent lack of selectivity is a major drawback and as such, a specific metal ion cannot be separated from others. In order to remove/separate a specific metal ion from a mixture, whether toxic or precious, a selective separation method is required. Selective separation of heavy metal ions is desirable not only from an environmental standpoint, but also as an economical one when the metal is precious or reusable.

An efficient method for selective separation is the ionic imprinting technique where the specific recognition capability is provided to the host molecules by addition and subsequent extraction of template molecules/ions [14–19]. Three steps are involved in the preparation of imprinted polymers: (i) mixing and self-assembling of template and polymerizable ligands into a complex; (ii) polymerization of this complex in the presence of a cross-linker; (iii) removal of the template after co-polymerization [20].

Recently, our group has developed a few types of copper-imprinted polymeric particles with different morphologies and imprinting positions ranging from bulk and surface imprinted to pore imprinted [21]. Particle size varied from 1 nm to 100 μm depending on the application modes. In those studies, the two-step reactions included preparation of the imprinted polymers, the synthesis of the ion containing the monomer, followed by its polymerization in the presence of a cross-linker. A single monomer with a functional ligand was used to provide the polymer with imprinting sites by binding and subsequent extraction of the template. Unlike the previous two-step synthetic methods, a single reaction step was involved in this research. To achieve reaction optimization, two types of functional monomers were used, one anionic and one cationic, that were simply blended with a copper template to form a metal/monomer complex by self-assembling through ionic interactions. The polymerization reaction of the copper/monomer complex, followed by extraction of the template, leads to the

* Corresponding author. Tel.: +82 31 290 7250 fax: +82 31 299 4700.
*E-mail address:* djkim@skku.edu (D. Kim).

0304-3894/$ – see front matter © 2009 Elsevier B.V. All rights reserved.
doi:10.1016/j.jhazmat.2009.08.107

production of the copper-imprinted particles. The structure and properties of the imprinted particles produced were analyzed using several techniques. The selective separation behavior of the present imprinted polymers was investigated in both batch and column separation modes, and the results were compared with those from commercial sources.

## 2. Experimental

### 2.1. Materials

The functional monomers of methacrylic acid (MAA) and 4-vinyl pyridine (4-VP), and the copper salt, $CuSO_4{\cdot}5H_2O$, were supplied from Sigma–Aldrich (Milwaukee, WI, USA). Ethylene glycol dimethacrylate (EGDMA), the cross-linker, was also supplied by Sigma–Aldrich. It was vacuum distilled for storage at 4 °C prior to use. Azobisisobutyronitrile (AIBN, Sigma–Aldrich) was used as an initiator and hydroxyethyl cellulose (HEC, Sigma–Aldrich) as a stabilizer in the polymerization reaction, respectively. All other chemical species were of reagent grade and purchased from Sigma–Aldrich. The water used in this experiment was de-ionized (DI water). Three types of commercial ion exchange resins were supplied from Bayer Chemicals (Germany): Lewatit monoplus S 100 of a strong acidic resin; Lewatit CNP 80 of a weak acidic resin; and Lewatit TP 207 of a chelating resin, respectively.

### 2.2. Synthesis of copper-imprinted polymer beads

The Cu(II)-imprinted polymer beads were prepared by a suspension polymerization technique. $Cu^{2+}$ aqueous solution was prepared by dissolving 2.5 mmol $CuSO_4{\cdot}5H_2O$ in 30 mL DI water. The functional monomers composed of MAA and VP, 5 mmol each, were added to $Cu^{2+}$ solution with continuous stirring until formation of the template($Cu^{2+}$)/monomer complex at pH around 4.0. EGDMA (cross-linker, 20 mmol), toluene (porogenic solvent, 10 mL) and AIBN (initiator, 2 wt.% based on vinyl monomers) were added and the resulting solution was mixed with 30 mL of 2 wt.% HEC (surfactant) aqueous solution. The polymerization reaction was carried out in a three-neck flask reactor equipped with a reflux condenser and nitrogen gas purge line, at 70 °C for 6 h with agitation at 250 rpm with constant nitrogen purging. The Cu(II)-containing polymer beads were collected after washing in an acetone:water (1:1) solution four times and dried *in vacuo* for 1 day. The Cu(II)-imprinted polymer beads were obtained after removal of the copper ions in solution using aqueous 1.0 M $HNO_3$ with vigorous agitation [22]. The non-imprinted polymer was also prepared for comparison in chemical structure, except without use of the $Cu^{2+}$ solution.

### 2.3. Chemical structure and morphology

Fourier transform infrared spectroscopy (Bruker IFS-66/S, FTIR, Bruker, USA) was used to identify the chemical structure of the polymers synthesized before and after extraction of the copper ions. The samples were prepared by blending the polymers and KBr crystals in powder form in a 1:100 mg weight ratio.

A scanning electron microscope (SEM, Philips Co., USA) was employed to investigate the size and morphology of copper-imprinted porous micro-beads. The samples were fractured under the quenched state in liquid nitrogen to observe interior morphology.

The surface area of the synthesized polymer beads was determined by a porosimetry analyzer (ASAP 2010, Micromeritics, Norcross, GA, USA) in a BET nitrogen adsorption and desorption mode after appropriate degassing and drying of the sample [23].

### 2.4. Batch separation analysis

The Cu(II)-imprinted polymer beads were used for batch separation analysis. In order to determine the copper adsorption capacity, 0.1 g of the Cu(II)-imprinted polymer beads were dissolved in 40 mL of the $Cu^{2+}$ aqueous solution at 10 ppm, at pH 6.2. In order to investigate the effect of the initial concentration of $Cu^{2+}$ solutions on adsorption capacity, the concentration of the Cu(II)-imprinted polymer beads in the $Cu^{2+}$ solutions was varied from 5 ppm to 100 ppm. The concentration of $Cu^{2+}$ solution was continuously measured using atomic absorption spectroscopy (AAS, Hitachi, Z-6100, Japan), with the adsorption capacity determined from the equilibrium concentration of the solution, until no further reduction of the $Cu^{2+}$ ion concentration was observed. Similar experiments were conducted at different pH's from 2 to 7 to investigate the effect on adsorption capacity. For selectivity studies, both 0.1 g Cu(II)-imprinted polymer beads and 0.1 g of commercial ion exchange resins were dissolved separately in 100 mL mixture solutions composed of $Cu^{2+}$, $Zn^{2+}$, and $Ni^{2+}$, 10 ppm each. The desorption kinetics test of Cu(II)-imprinted polymer beads was carried out using 500 mL of 1 M $HNO_3$ solution as a desorption medium. The content of $Cu^{2+}$ ions desorbed from Cu(II) occupied polymer particles was determined measuring the $Cu^{2+}$ concentration in the desorption medium using AAS at each time.

### 2.5. Column separation analysis

The Cu(II)-imprinted polymer beads, 2.0 g, were packed into the column (Alltech, Threaded SS, 4.6 mm id × 250 mm height) using a column packer (Alltech, model 1666, USA) for column separation analysis. DI water was passed through the packed column with a volume five times that of the column. After the washing process with DI water, a metal ion mixture composed of $Cu^{2+}$, $Zn^{2+}$, and $Ni^{2+}$, each at 10 ppm, was passed through the column at a flow rate of 2 mL/min. The outlet solution from the column was periodically collected to measure the concentration of each metal ion by AAS. The column separation experiment was conducted at pH 6.2.

## 3. Results and discussion

### 3.1. Synthesis of $Cu^{2+}$-imprinted polymer beads

In this polymer synthesis, the metal-bound monomer was not necessarily pre-synthesized. Instead, two types of monomers, methacrylic acid and 4-vinyl pyridine, were used. In order to provide strong imprinting sites, the solid binding of the template ion to the monomer ligand is a prerequisite. An ionic complex can be established between the cationic copper ion and anionic carboxylic acid ligand in methacrylic acid *via* ionic interactions, but its strength is actually insufficient as the dissociation of the carboxylic acid is not favored in water. Although 4-vinyl pyridine itself possibly forms the coordination complexes with copper ions, its presence promotes the complex formation between the carboxylic acid and copper ion by acting as a base and aiding in the dissociation of the carboxylic groups through proton abstraction, as depicted in Fig. 1. The synthesis of the imprinted polymer performed by such a single step reaction simplifies its production process and provides superb imprinting capabilities.

The synthesis of $Cu^{2+}$-imprinted polymer beads was assured from the FTIR spectra measured for the polymers before and after extraction of the template ion. As shown in Fig. 2, the characteristic IR band arising from Cu–O bonding at 1610 $cm^{-1}$ was clearly observed for the polymers before removal of the Cu ions, but no band at this position was observed for those Cu-imprinted (removed) [21]. The IR spectrum of the Cu-imprinted (removed)

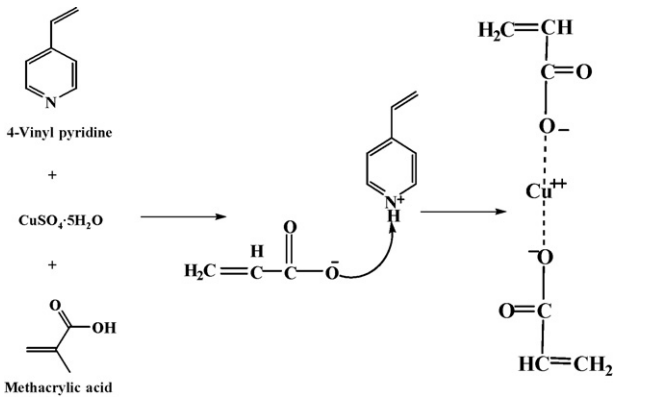


**Fig. 1.** Schematic representation of the complex formation between the copper ion and functional monomers.

polymer was the same as that of the non-imprinted polymer. The characteristic band of pyridine ring was observed at 1638 $cm^{-1}$.

The size and shape of copper-imprinted polymer particles measured by SEM are shown in Fig. 3. The beads were near 250 μm and spherical in shape. The pores in the beads facilitated the diffusion of the metal ions, owing to a high internal surface area, enhancing the adsorption property capacities of MIP.

The surface area, total pore volume, and pore width were determined for the copper-imprinted polymer, along with the three commercial resins. As shown in Table 1, the copper-imprinted polymer possessed a larger surface area (60.5 $m^2/g$) than the commercial resins, indicating its highly porous structure. The total pore volume of the copper-imprinted polymer was 0.14 $cm^3/g$, also much higher than the commercial resins. The average pore width of the $Cu^{2+}$-imprinted polymer, however, is in-between two of the commercial resins (weak acid resin and chelating resin).

### 3.2. Batch separation characteristics

Fig. 4 shows the pH dependence of adsorption capacity of the $Cu^{2+}$-imprinted polymer beads. Adsorption capacity, $Q$ is defined by Eq. (1):

$$Q = \frac{\text{The total amount of adsorbed metal ions}}{\text{The used mass of the imprinted beads}} \quad (1)$$

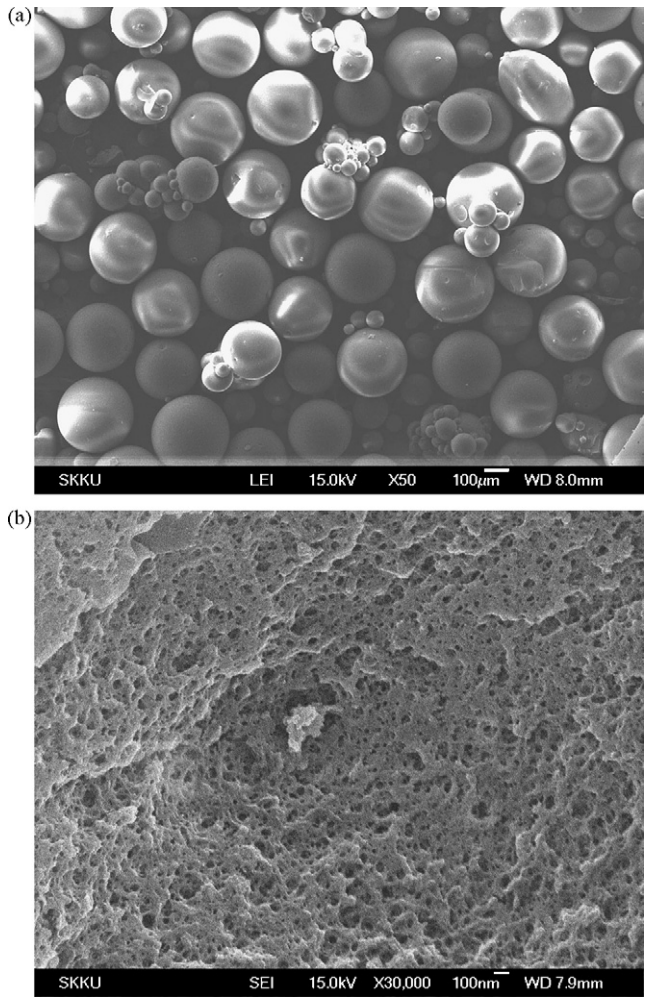


**Fig. 3.** SEM images of (a) exterior and (b) interior of Cu(II)-MIIP, respectively.

A decrease in pH results in the reduction of the adsorption capacity because the copper-imprinted sites of the polymer are occupied by protons rather than copper ions in an acidic environment. The maximum adsorption capacity was observed around pH 6.5, without further increase.

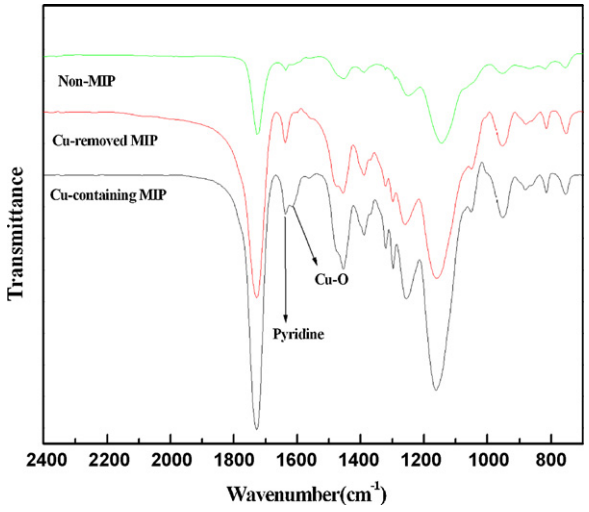


**Fig. 2.** FTIR spectra of non-MIIP, Cu(II)-removed MIIP and Cu(II)-containing MIIP, respectively.

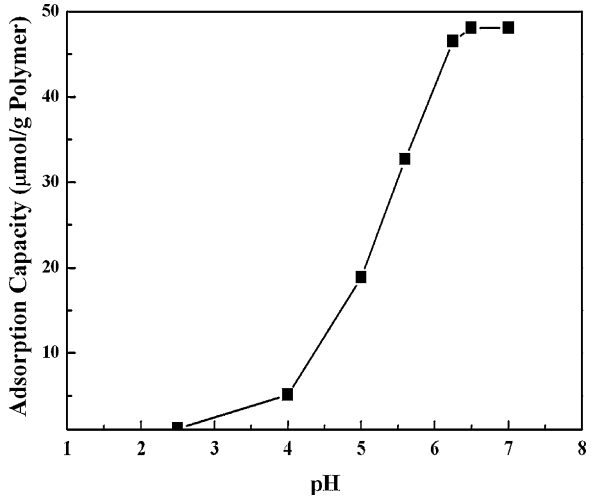


**Fig. 4.** Effect of pH on the adsorption capacity of Cu(II)-MIIP particles. Initial concentration of metal solution was 10 ppm.

**Table 1**
Surface area, total pore volume, pore size width, and selectivity coefficients of Cu(II)-MIIP and commercialized ion exchange resins.

| | BET measurement | | | Selectivity coefficient | |
|---|---|---|---|---|---|
| | BET surface area ($m^2$/g) | Total pore volume ($cm^3$/g) | Average pore width (nm) | $\alpha(D_{Cu}/D_{Ni})$ | $\alpha(D_{Cu}/D_{Zn})$ |
| Cu(II)-MIIP | 60.5 | 0.14 | 9.16 | 43.48 | 42.38 |
| Strong acid resin (Lewatit monoplus S100) | 0.013 | N/D | N/D | 1.06 | 1.04 |
| Weak acid resin (Lewatit CNP 80) | 1.57 | 0.000138 | 2.07 | 4.85 | 3.35 |
| Chelating resin (Lewatit TP207) | 8.58 | 0.047 | 21.4 | 1.08 | 1.11 |

The effect of particle size on the adsorption capacity was also examined. The amount of copper adsorption at equilibrium slightly increased with decreasing particle size because the surface area increased with decreasing particle size. Larger surface areas provide more binding sites for surrounding metal ions.

In Fig. 5(a) and (b), the adsorption kinetics of the copper-imprinted and non-imprinted polymer beads are shown for $Cu^{2+}$, $Zn^{2+}$, and $Ni^{2+}$, respectively. For the copper-imprinted polymer beads, copper ions are adsorbed on polymer beads much faster than other metal ions, and their adsorption capacity is also much higher than other metal ions. For the non-imprinted polymer beads, however, no selective separation behavior for template ion is observed, as all metal ions involved are absorbed on polymer beads to the almost same degrees. From this observation, higher selective and faster adsorption behavior of the imprinted polymer for the template metal ion is expected.

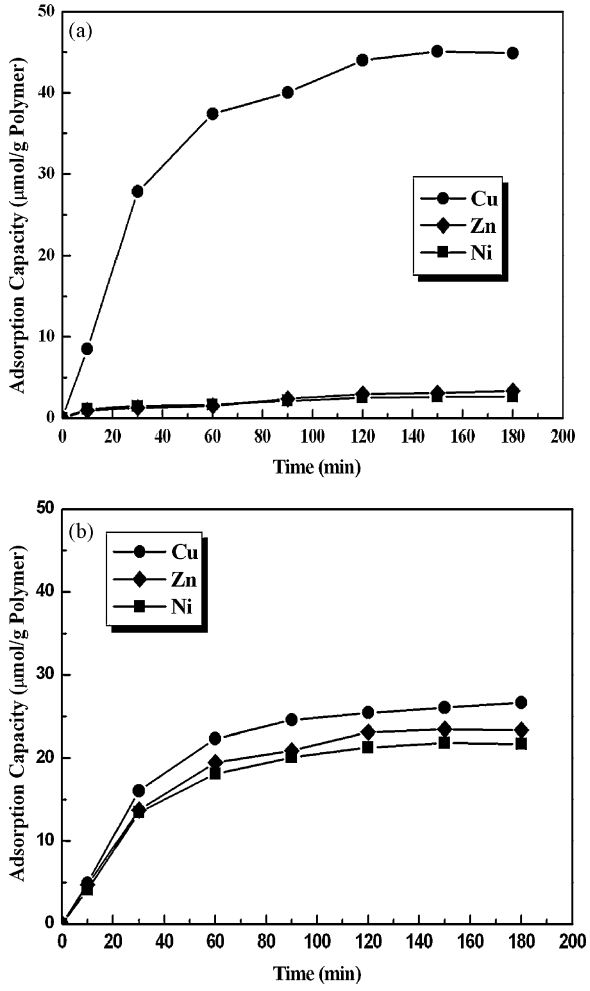


**Fig. 5.** Adsorption kinetics of Cu(II), Zn(II), and Ni(II) ions on the (a) Cu(II)-MIIP and (b) non-MIIP particles.

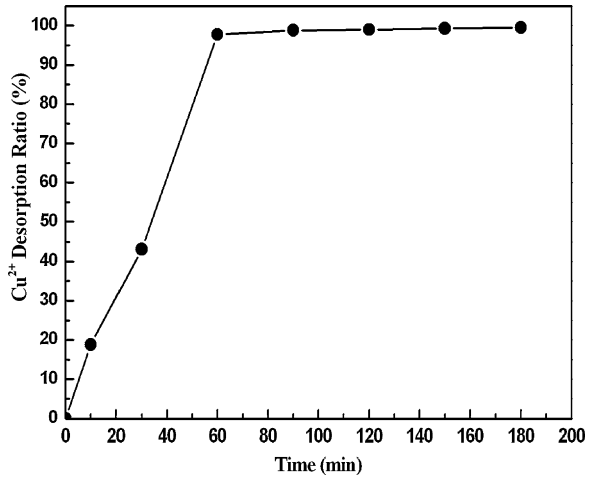


**Fig. 6.** Desorption kinetics of Cu(II) metal ion from Cu(II)-MIIP particles.

Fig. 6 shows the desorption kinetics of copper-imprinted polymer beads for the copper ion. The desorption percentage reached almost 100% after 60 min at equilibrium. As the copper ions can be completely removed from the polymer particles by desorption process in relatively short time, those can be used repeatedly without significant loss of adsorption capacity. The desorption ratio, $Q'$ is defined by Eq. (2):

$$Q' = \frac{\text{The desorbed amount of metal ions}}{\text{The adsorbed amount of metal ions in the imprinted beads}} \quad (2)$$

Fig. 7 shows the feed concentration effect on the adsorption capacity for the copper ion. The adsorption capacity increases with feed copper ion concentration in a linear fashion until equilibrium,

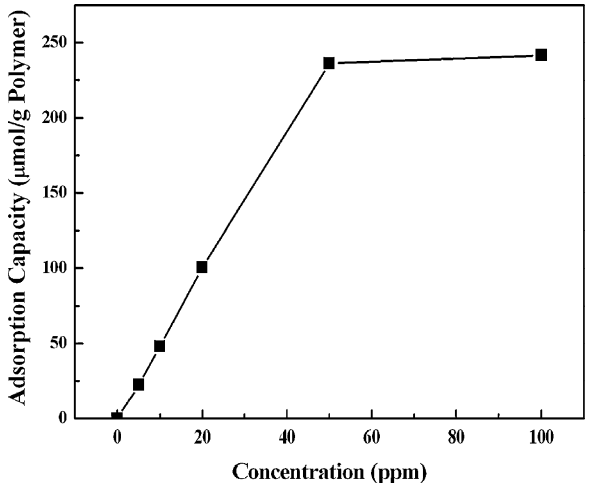


**Fig. 7.** Effect of initial concentration of copper ion on the adsorption capacity of Cu(II)-MIIP particles at pH 6.2.

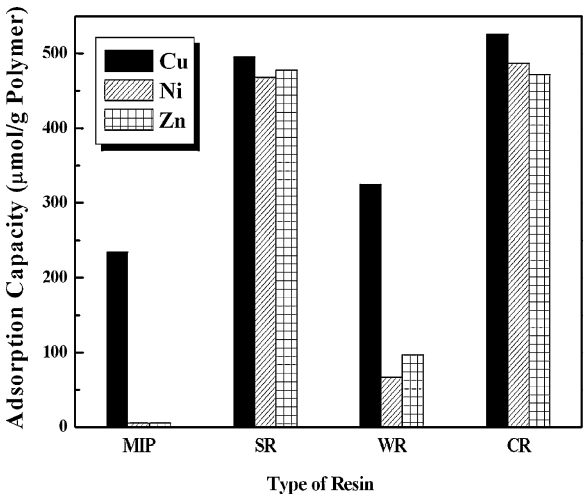


**Fig. 8.** Comparison of adsorption capacity between MIIP and commercial ion exchange resins: SR (strong acid resin), WR (weak acid resin), and CR (chelating resin) for Cu(II), Ni(II), and Zn(II) ions.

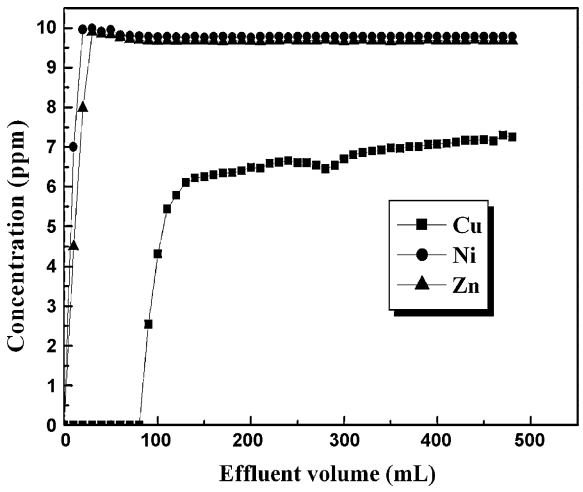


**Fig. 9.** The column adsorption behavior of Cu(II)-MIIP particles for Cu(II), Ni(II), and Zn(II) ions at pH 6.2. Feed flow rate was 2 mL/min.

where no further copper ions are adsorbed onto the polymer beads as all binding sites have become saturated. From this equilibrium adsorption behavior, it is recognized that the maximum capacity of the present copper-imprinted polymer beads is 235 μmol/g polymer.

Fig. 8 shows the adsorption properties of MIIP and commercial resins for comparison. The chelating resin has the highest adsorption capacity for all metal ions. The adsorption capacity of MIP for the copper ion is a slightly lower than those of commercial polymers, however, the difference between it and other metal ions such as Ni(II) and Zn(II) is significant. While little of the Ni(II) and Zn(II) ions are adsorbed onto the copper-imprinted resins, large amounts of Ni(II) and Zn(II) are still adsorbed on the commercial resins, indicating that the Cu(II)-MIIP has a much stronger affinity for $Cu^{2+}$ than other metal ions.

The adsorption behavior of MIIP was analyzed according to adsorption isotherms. The most widely used isotherm equation in modeling adsorption behavior is the Langmuir equation. Assuming that the entire binding site can only adsorb one molecule and be energetically equivalent, and that there is no interaction among adsorbed molecules, the Langmuir adsorption equation [5] is given by Eq. (3):

$$Q = \frac{Q_{max} b C_e}{1 + b C_e} \tag{3}$$

where $Q$ is the adsorbed metal ion quantity per unit weight of MIIP at equilibrium (μmol/g), $C_e$ the un-adsorbed Cu(II) ion concentration in solution at equilibrium (μmol/L), $b$ the Langmuir constant (g/μmol), and $Q_{max}$ the maximum adsorption capacity (μmol/g), respectively.

All parameters in the Langmuir equation were estimated from experimental data. The values of $Q_{max}$ and $b$ were determined from the intercept and slope of the Langmuir plot [24]. The maximum adsorption capacity ($Q_{max}$) of MIIP was founded to be 254 μmol/g, very similar to the experimental polymer, 235 μmol/g. The Langmuir adsorption model can be applied to this system at a correlation coefficient ($R^2$) of 0.9654.

### 3.3. Column separation analysis

Fig. 9 shows the selective adsorption behavior of the copper-imprinted polymer when the Cu(II), Ni(II), and Zn(II) ion mixture was fed into the column. For zinc and nickel ion adsorption, the outlet concentration abruptly increased to equilibrium (the same as feed concentration) within 10 min after injection. The copper adsorption behavior of Cu(II)-MIIP was, however, quite different from other metal ions. The outlet concentration increased after 40 min and reached 70% of the initial concentration after 60 min, followed by a slight increase to equilibrium, indicating a preferential binding property of Cu(II)-imprinted polymers for Cu(II) ions. As the binding capacity decreases when numerous imprinting sites have been occupied by Cu(II) ions, a slow adsorption is observed from about 60 min. The adsorption quantity of Cu(II)-MIIP was determined by integrating the curve showing the relationship between adsorption quantity (μmol/mL) and effluent volume (mL). The adsorption quantity of Cu(II)-MIIP was found to be 17.50 μmol/g, up to an effluent volume of 480 mL.

The selectivity coefficient for a copper ion in the presence of other ion species was determined from Eq. (4):

$$\alpha = \frac{D_{Cu}}{D_M} \tag{4}$$

$$D = \frac{C_A - C_B}{C_A} \times \frac{v}{m} \tag{5}$$

Here, $v$ is the volume of the solution (mL) and $m$ the mass of the polymer (g), with $C_A$ and $C_B$ the initial and final concentrations of the metal ions (mg/L), respectively. $D_{Cu}$ and $D_M$ represent the distribution ratios of $Cu^{2+}$ and one of the other metal ions, respectively [21].

Table 1 shows the resulting selectivity of copper-imprinted polymer beads for copper, zinc, and nickel ions, respectively. The selectivity coefficient for copper ion is 42.48 times higher than Zn, and 43.48 times that of Ni, respectively, with the present imprinted polymers having a copper selectivity at least 10 times higher than those from commercial sources.

## 4. Conclusions

Copper (II) ion-imprinted porous polymer micro-particles with an average diameter of 250 μm were prepared using two functional monomers, MAA and VP. The surface area of the particles was enlarged *via* pore formation (BET 60 $m^2$/g) using a toluene porogenic agent. The adsorption properties of the Cu(II)-MIIP showed a high affinity for $Cu^{2+}$ over NI(II) and Zn(II) ions through batch and column analysis. The adsorption capacity of the prepared MIIP was slightly lower than those from commercial sources, but the selective separation capability for the template Cu(II) ion was much higher than those from commercial sources. From this

equilibrium adsorption behavior, the maximum capacity of the copper-imprinted polymer beads was 235 μmol/g polymer. The selectivity coefficient for the copper ion was 42.48 times that of Zn, and 43.48 times that of Ni, respectively, with the present imprinted polymers having a copper selectivity at least 10 times higher than those from commercial sources.

## Acknowledgments

This work was supported by the Core Environmental Technology Development Project for the Next Generation of the Korea Institute of Environmental Science and Technology (KIEST) (Grant # 022-081-048).

## References

[1] M. Devi, M. Fingermann, Inhibition of acetylcholinesterase of activity in the central nervous system of the red swamp crayfish, procambarus clarkia, by mercury, cadmium, and lead, Bull. Environ. Contam. Toxicol. 55 (1995) 746–750.
[2] R.A. Beuvais, S.D. Alexandratos, Polymer-supported reagents for the selective complexation of metal ions: an overview, React. Funct. Polym. 36 (1998) 113–123.
[3] B.L. Rivas, S.A. Pooley, H.A. Maturana, S. Villegas, Metal ion uptake properties of acrylamide derivatives of resins, Macromol. Chem. Phys. 202 (2001) 443–447.
[4] B.E. Reed, W. Lin, M.R. Matsumoto, J.N. Jensen, Physicochemical processes, Water Environ. Res. 69 (1997) 444–462.
[5] A. Kara, L. Uzun, N. Besirli, A. Denizli, Poly(ethylene glycol dimethacrylate-n-vinylimidazole)beads for heavy metal removal, J. Hazard. Mater. 106B (2004) 93–99.
[6] L. Wu, Y. Li, Picolinamide-Cu(Ac)2-imprinted polymer with high potential for recognition picolinamide-copper acetate complex, Anal. Chim. Acta 482 (2003) 175–181.
[7] B. George, V.N.R. Pillai, B. Mathew, Effect of the nature of the crosslinking agent on the metal-ion characteristics of 4 mol% DVB- and NNMBA-crosslinked polyacrylamide-supported glycines, J. Appl. Polym. Sci. 74 (1999) 3432–3444.
[8] M. Chanda, G.L. Rempel, Chromium(III) removal by poly(ethyleneimine) granular sorbents made by a new process of templated gel filling, React. Funct. Polym. 35 (1997) 197–207.
[9] J.L. Suarez-Rodrıguez, M.E. Dıaz-Garcıa, Flavonol fluorescent flow-through sensing based on a molecular imprinted polymer, Anal. Chim. Acta 405 (2000) 67–76.
[10] T.-Y. Guo, Y.-Q. Xia, J. Wang, M.-D. Song, B.-H. Zhang, Collection of neutral inducing factors from PA6 cells using heparin solutions and their immobilization on plastic culture dishes for induction of neutrons from embryonic stem cells, Biomaterials 26 (2005) 5737–5745.
[11] D. Cunliffe, A. Kirby, C. Alexander, Molecularly imprinted drug delivery systems, Adv. Drug Del. Rev. 57 (2005) 1836–1853.
[12] D.L. Rathbone, Molecularly imprinted polymers in the drug discovery process, Adv. Drug Del. Rev. 57 (2005) 1854–1874.
[13] A.L. Hillberg, K.R. Brain, C.J. Allender, Molecularly imprinted polymer sensors: implication for therapeutics, Adv. Drug Del. Rev. 57 (2005) 1875–1889.
[14] R. Kara, J.V. Biju, T.P. Rao, Influence of binary/ternary complex of imprint ion on the preconcentration of uranium(IV) using ion imprinted polymer materials, Anal. Chim. Acta 512 (2004) 63–73.
[15] P.G. Krishna, J.M. Gladis, T.P. Rao, G.R. Naidu, Selective recognition of neodymium (III) using ion imprinted polymer particles, J. Mol. Recognit. 18 (2005) 109–116.
[16] I. Dakova, I. Karadjova, I. Ivanov, V. Georgieva, B. Etimova, G. Georgiev, Solid phase selective separation and preconcetration of Cu(II) by Cu(II)-imprinted polymethacrylic microbeads, Anal. Chim. Acta 584 (2007) 196–203.
[17] C.R. Preetha, J.M. Gladis, T.P. Rao, Removal of toxic uranium from synthetic nuclear power reactor effluents using uranyl ion imprinted polymer particles, Env. Sci. Technol. 40 (2006) 3070–3074.
[18] N.T. Greene, K.D. Shimizu, Colorimetric molecularly imprinted polymer sensor array using dye displacement, J. Am. Chem. Soc. 127 (2005) 5695–5700.
[19] M. Trojanowicz, W. Marzena, Electrochemical and piezoelectric enantioselective sensors and bioselective sensors, Anal. Lett. 38 (2005) 523–547.
[20] M. Shamsipur, J. Fasihi, A. Khanchi, R. Hassani, K. Alizadeh, H. Shamsipur, A stoichiometric imprinted chelating resin for selective recognition of copper(II) ions aqueous media, Anal. Chim. Acta 599 (2007) 294–301.
[21] H.A. Dam, D. Kim, Metal ion imprinted polymer microspheres derived from copper methacrylate for selective separation of heavy metal ions, J. Appl. Polym. Sci. 108 (2008) 14–24.
[22] T. Rohr, S. Knaus, H. Gruber, D.C. Sherrington, Preparation and porosity characterization of highly-crosslinked polymer resins derived from multifunctional (meth)acrylate monomers, Macromolecules 35 (2002) 97–105.
[23] N. Gupta, A.K. Srivastava, Interpenetrating polymer networks (IPNs) from poly(methacrylates): synthesis and properties, Macromolecules 28 (1995) 827–832.
[24] Y. Sağ, B. Akcael, T. Kutsal, Evaluation, interpretation, and representation of three metal biosortion equilibria using a fungal biosorbent, Proc. Biochem. 37 (2001) 35–50.